scientific reports

Check for updates

OPEN

Action inflexibility and compulsive-like behavior accompany neurobiological alterations in the anterior orbitofrontal cortex and associated striatal nuclei

Laura M. Butkovich[1,2], Sophie T. Yount[1,2,3], Aylet T. Allen[1,2], Esther H. Seo[1,2], Andrew M. Swanson[1,2,4] & Shannon L. Gourley[1,2,3,4]✉

The orbitofrontal cortex (OFC) is a large cortical structure, expansive across anterior-posterior axes. It is essential for flexibly updating learned behaviors, and paradoxically, also implicated in inflexible and compulsive-like behaviors. Here, we investigated mice bred to display inflexible reward-seeking behaviors that are insensitive to action consequences. We found that these mice also demonstrate insensitivity to Pavlovian-to-instrumental transfer, as well as compulsive-like grooming behavior that is ameliorated by fluoxetine and inhibitory, but not excitatory, chemogenetic modulation of excitatory OFC neurons. Thus, these mice offer the opportunity to identify neurobiological factors associated with inflexible and compulsive-like behavior. Experimentally bred mice suffer excitatory dendritic spine attrition, as well as changes in inhibitory synapse-associated proteins, GAD67/GAD1 and SLITRK3, largely in the anterior and not posterior OFC (or medial frontal cortex). They also display higher levels of the excitatory synaptic marker striatin in the nucleus accumbens and lower levels of the excitatory synaptic marker SAPAP3 in the dorsal striatum, striatal nuclei that receive input from the anterior OFC. Together, our findings point to the anterior OFC as a potential locus controlling action flexibility and compulsive-like behavior alike.

Keywords Orbital, SAPAP3, Grooming, Ventral striatum, Habit, Compulsivity

The orbitofrontal cortex (OFC) is a large cortical brain region located at the base of the frontal cortex. It controls flexible reward-seeking behavior particularly when organisms must infer the possible outcomes of their actions and favor a given action plan over another[1–4]. Interestingly, it is also implicated in repetitive actions resembling habitual and compulsive-like behavior – behaviors seemingly occurring in the absence of action strategizing or inhibitory control. For example, chemogenetic, optogenetic, and pharmacological stimulation or disinhibition of excitatory OFC neurons induces habit- and compulsive-like behavior in rodents[2,5–9] and impedes the ability of organisms to use information regarding prior actions to inform future behavior[10]. In humans, gene transcripts associated with both excitatory and inhibitory neurotransmission differ in the OFC between individuals with and without obsessive-compulsive disorder (OCD)[11].

The OFC can be divided along the anterior-posterior and medial-lateral axes[12]. The anterior ventrolateral OFC (aVLO) appears to be particularly involved in updating reward-seeking behavioral response strategies, while the posterior (p) VLO is not[2]. Similar motifs were recently identified in the medial OFC (MO), in that the aMO is necessary for value inference and suppressing responding for non-valued outcomes, while the pMO is not[13]. These patterns suggest that one potential explanation for the apparent dissociation in OFC function – coordinating response flexibility and habit-biased and compulsive-like behaviors alike – may be that the anterior vs. posterior regions are associated with different behavioral domains. Alternatively, distinctive molecular features within a given subregion may distinguish organisms biased towards flexible goal-seeking behavior vs. those who are less flexible and/or prone to compulsive-like behaviors.

[1]Department of Pediatrics, Children's Healthcare of Atlanta, Emory University School of Medicine, Atlanta, GA, USA. [2]Emory National Primate Research Center, Emory University, 954 Gatewood Rd. NE, Atlanta, GA 30329, USA. [3]Graduate Program in Molecular and Systems Pharmacology, Emory University, Atlanta, GA, USA. [4]Graduate Program in Neuroscience, Emory University, Atlanta, GA, USA. ✉email: Shannon.l.gourley@emory.edu

To investigate this conceptual framework, we required a mouse model that displays action inflexibility and compulsive-like behavior. To this end, we recently screened large populations of mice for their capacity to modify learned behaviors when those behaviors failed to be rewarded. We bred mice that performed poorly, demonstrating inflexible action. Their offspring demonstrated the same inflexible response propensities[14]. These mice provide a tool by which to ask: (1) Do mice demonstrating poor action flexibility also demonstrate compulsive-like behavior? (2) Do these mice suffer changes in the neurobiological milieu of the OFC? (3) And are any changes localized to the anterior vs. posterior regions?

While no animal model can be considered an exact model of any particular human condition, self-grooming in rodents has value in the context of studying compulsion[15]. Self-grooming is an innate behavior that includes highly conserved, stereotyped action sequences, and is one of the most frequently performed behaviors in rodents[16]. Both spontaneous and elicited self-grooming are measured in mouse models for studying compulsion. In the spray-elicited self-grooming assay, mice are sprayed with water and placed in a novel environment. Typical mice will divide time between exploring and grooming. Mice prone to compulsive-like behavior demonstrate more grooming at the expense of exploring the novel (potentially threatening) environment. Self-grooming involves a distributed neural circuitry, including brainstem circuits and higher-order structures involved in the motor control and sequencing of the behavior[16]. These structures include the basal ganglia and associated nuclei, and even amygdalar and cortical structures like the OFC[16,17].

We find that mice bred to display action inflexibility demonstrate intensive self-grooming, as well as amphetamine-elicited repetitive behavior. To identify neurobiological correlates, we examined a constellation of proteins that are: (1) implicated in synaptic strength and number, and (2) amenable to visualization by immunostaining, which allowed us to investigate their levels along the anterior-posterior axis of the small mouse brain. We also visualized and classified dendritic spines, the primary sites of excitatory plasticity in the brain, along the anterior-posterior axis. In sum, mice bred to display inflexible and compulsive-like behavior suffer changes in both excitatory and inhibitory synapse-associated markers in the VLO and overwhelmingly, in the anterior region. The anterior OFC richly innervates striatal output structures – providing one avenue by which it controls action flexibility and compulsive-like behavior alike.

Results

Recently, we identified and bred mice that spontaneously fail to modify trained behaviors when expected rewards are withheld[14]. Instead, they persist in responding, favoring habitual behaviors, which are insensitive to reward delivery[18]. Their progeny and their progeny's progeny also fail to modify their actions flexibly. Hence, we have created a line of mice with poor ability to engage in goal-directed behaviors; they instead defer to habit-like behaviors, which are inflexible and insensitive to action-outcome contingencies. Here we investigated this line of mice, referred to as EB (experimentally bred) mice, to test the hypothesis that action inflexibility would associate with compulsive-like behavior and changes in OFC neurobiology. Throughout, control mice were same-age, same-strain offspring of independent parents who were not themselves subject to experimental breeding.

The task used to identify mice for breeding and to validate the efficacy of experimental breeding was as follows: We tested mice in operant conditioning chambers containing 3 nose poke ports, and a separate food magazine where reinforcers were delivered. Two of the nose poke ports were active during training, meaning responding was reinforced, while a third was inactive, meaning responses had no programmed consequences (Fig. 1a). Next, one active port was physically occluded, and responses on the remaining port continued to be reinforced (Fig. 1a, center). The following day, the other previously active port was made available, but pellets were delivered noncontingently, or "for free," independently of nose pokes (Fig. 1a, bottom). The third, always inactive port was available throughout. Mice that can flexibly update their action strategy are expected to inhibit responding when pellets are given noncontingently, since their responding is not causing the food to be delivered.

In comparing control and the offspring of EB mice, all mice were able to learn to nose poke during training (Fig. 1b; main effect of session: $F_{(6,132)} = 52.214$, $p < 0.001$), responding more on the active vs. inactive ports (interaction session*port: $F_{(6,132)} = 27.731$, $p < 0.001$), with no difference between groups (no main effect of group: $F_{(1,22)} = 3.146$, $p = 0.090$; no interaction group*port: $F_{(1,22)} = 2.211$, $p = 0.151$; no interaction group*session: $F_{(6,132)} = 1.227$, $p = 0.297$). When one response then failed to be reinforced, control mice adjusted their behavior, inhibiting that response such that rates were equivalent to the always inactive port – evidence that they recognized that responding was not reinforced (Fig. 1c; interaction group*session*port: $F_{(1,22)} = 4.317$, $p = 0.05$; posthoc ctrl responses during non-reinforced session on active vs. inactive port: $t_{(11)} = 0.054$, $p = 0.956$; ctrl responses during reinforced session: $t_{(11)} = 6.148$, $p < 0.001$). Meanwhile, EB mice were inflexible, responding equivalently during the reinforced vs. non-reinforced conditions. In fact, even though their responding was not reinforced, they persisted in it, generating response rates above those on the third, always inactive port (Fig. 1c; posthoc EB responses during non-reinforced session on active vs. inactive port: $t_{(11)} = 2.717$, $p = 0.020$; EB responses during reinforced session: $t_{(11)} = 7.731$, $p < 0.001$).

Failures in response inhibition could not obviously be attributable to hedonic responses to food or locomotor activity, given that food magazine entries did not differ by group (Fig. 1d; no interaction group*session: $F_{(1,22)} = 1.176$, $p = 0.290$; no main effect of group: $F_{(1,22)} = 1.452$, $p = 0.241$; no main effect of session: $F_{(1,22)} = 3.576$, $p = 0.0719$). Ambulatory activity across 24 h also did not differ between groups (Fig. 1e; no interaction group*time: $F_{(23,299)} = 0.840$, $p = 0.680$; no main effect of time: $F_{(6.603,85.84)} = 1.784$, $p = 0.105$; no main effect of group: $F_{(1,13)} = 2.548$, $p = 0.135$).

We next examined whether deficits in action flexibility extended beyond changes in the predictive relationship between responses and their outcomes. In a separate cohort of mice, we used a Pavlovian-to-instrumental transfer test (Fig. 1f) conducted in conditioning chambers containing 2 inset lights, an extendable lever, a house light, and a separate food magazine. During Pavlovian conditioning, pellets were delivered in the presence of one light, which served as the conditioned stimulus (CS+). Meanwhile, the other light signaled no pellet

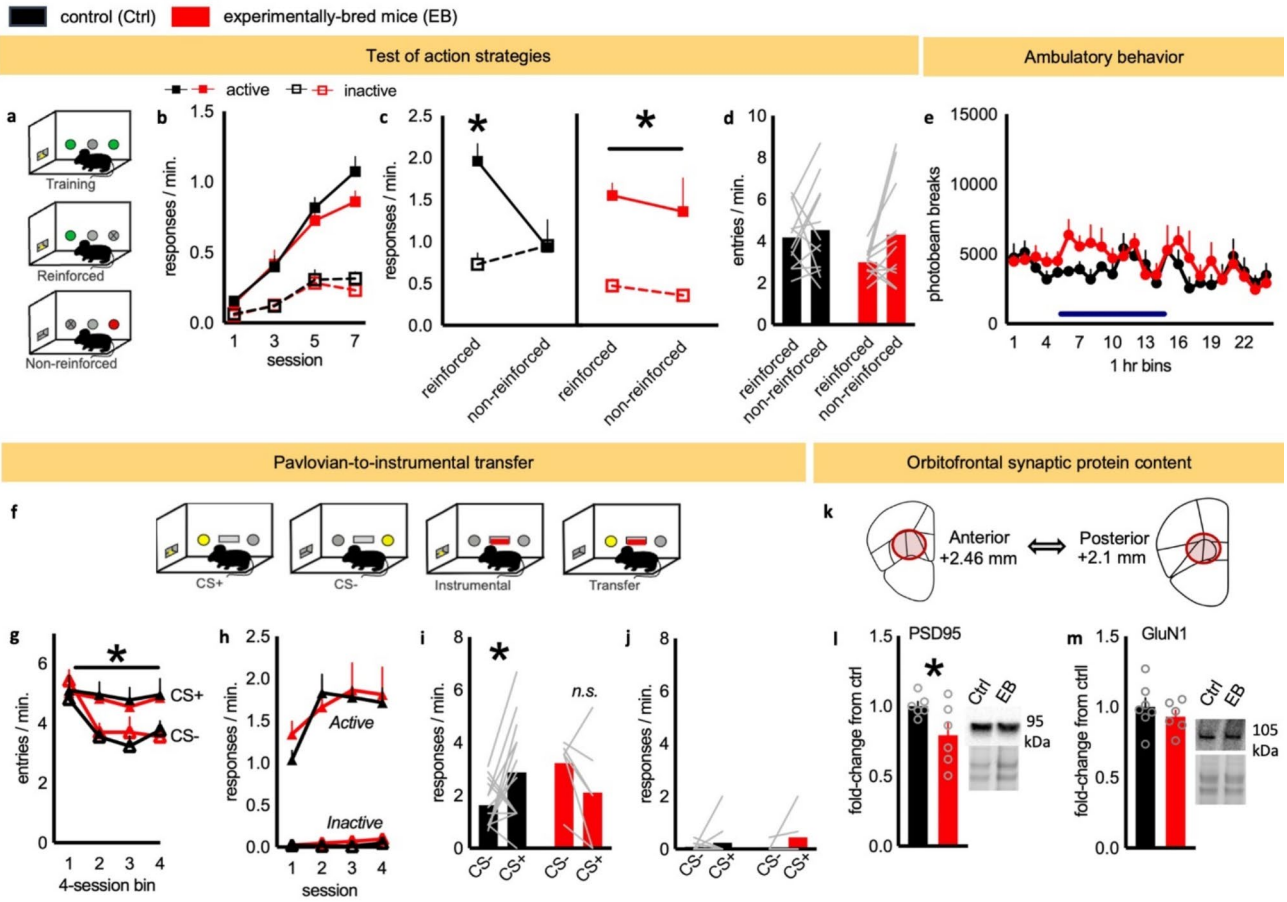

Fig. 1. Action inflexibility and synaptic marker loss in the VLO following selected breeding. (**a**) Task schematic. Responding on two lateral nose poke ports (green), but not a center inactive port (gray) resulted in food pellet delivery in a separate food magazine. Next, in the reinforced session, one nose poke port was physically occluded, while responding on the available active nose poke port remained reinforced. In the non-reinforced session, the opposite nose poke port was occluded. Here, responding on the available nose poke port was not reinforced, with food pellets instead delivered non-contingently. The center, inactive port was available throughout. (**b**) Ctrl and EB mice acquired the nose poke responses, distinguishing between the 2 active ports over the inactive third port ($n = 12$/group). (**c**) Next, ctrl mice responded more during the reinforced session than non-reinforced session, with response rates on the always-inactive port remaining low throughout. In EB mice, however, response rates did not differ between reinforced and non-reinforced conditions (right). (**d**) Food magazine entries and (**e**) ambulatory activity ($n = 8$ ctrl, 7 EB) did not differ between groups. Blue bar represents time with lights off. (**f**) Task schematic. Mice were trained to associate one light (the conditioned stimulus, CS+) with food and another (CS-) with no food. Separately, mice were trained to press a lever for the same food. During the transfer test, the CS + and CS- were presented with the lever ($n = 14$ ctrl, 6 EB). (**g**) During Pavlovian training, mice entered the magazine more during the CS+, with no group differences. (**h**) During instrumental conditioning, mice generated food-reinforced lever presses (active response) and neglected non-reinforced nose poke ports that contained the stimulus lights (inactive response), again with no group differences. (**i**) During the transfer test, control mice responded more during the CS+, while EB mice did not. (**j**) Approaches to the CS ports were uniformly low during the transfer test. (**k**) Schematic images and Bregma measurements from *The Mouse Brain in Stereotaxic Coordinates*[62] representing the location and anterior-posterior extent of samples collected from the VLO by tissue punch. (**l**) EB mice had lower PSD95 levels in the VLO than ctrl mice ($n = 6$/group), with no changes in (**m**) GluN1 (ctrl $n = 7$, EB $n = 6$). Representative blots, cropped at the appropriate molecular weights, and total protein inset shown. Full gels are shown in Fig. S3-4. Proteins were detected at the expected weights. Data shown as mean + SEM, or fold-change from control mean + SEM for western blots, with bars and connected symbols representing means and individual symbols and gray lines representing individual mice. $^*p \leq 0.05$.

delivery (CS-). Over time, mice entered the food magazine more often during the CS + than CS- (Fig. 1g; CS: $F_{(1,18)} = 13.121$, $p = 0.002$; interaction session*CS: $F_{(3,54)} = 4.903$, $p = 0.004$; no main effect of group: $F_{(1,18)} = 0.019$, $p = 0.893$), indicating that all mice could discriminate between the CSs.

Next, mice were trained to press a previously retracted lever for food (Figs. 1f and 3rd panel). The lights were extinguished, and approaching the ports that contained them had no programmed consequences. Over time,

all mice differentiated between the lever press (active) responses and approaching the light ports (inactive); i.e., they learned to lever press for food (Fig. 1h; interaction session*response: $F_{(3,54)} = 6.291$, $p < 0.001$; main effect of response: $F_{(1,18)} = 175.425$, $p < 0.001$; no main effect of group: $F_{(1,18)} = 0.030$, $p = 0.864$).

The final component was the transfer test when, for the first time, the lever was extended in the presence of the CS + or CS- (Fig. 1f, far right). Both groups lever-pressed, but control mice pressed more during the CS+ – demonstrating the transfer effect – while EB mice did not (Fig. 1i; interaction CS*group: $F_{(1,18)} = 6.308$, $p = 0.022$; posthoc comparison of ctrl CS responses: $t_{(13)} = 2.334$, $p = 0.036$; comparison of EB CS responses: $t_{(5)} = 1.567$, $p = 0.178$). Regardless of group, mice generated virtually no approaches to the CS's (Fig. 1j; no interaction CS*group: $F_{(1,18)} = 0.418$, $p = 0.526$; no main effect of CS: $F_{(1,18)} = 2.61$, $p = 0.124$; no main effect of group: $F_{(1,18)} = 0.411$, $p = 0.530$).

Altogether, EB mice are unable to interleave new information into established behavioral response strategies, a function commonly attributed to the VLO. Thus, in a separate group of mice, we next examined levels of canonical excitatory synaptic proteins using western blot of gross tissue punches spanning the anterior-posterior axis (Fig. 1k). Post-synaptic density protein 95 (PSD95), a post-synaptic scaffolding protein highly expressed in glutamatergic synapses, was lower in EB mice (Fig. 1l; $t_{(10)} = 2.181$, $p = 0.05$). Meanwhile, the obligatory NMDA receptor subunit GluN1 was unchanged (Fig. 1m; $t_{(11)} = 0.877$, $p = 0.399$).

Breeding mice for poor action flexibility results in dendritic spine attrition in the VLO and compulsive-like behavior

Based on this pattern of PSD95 loss in the OFC, we visualized dendritic spines, the primary sites of excitatory synapses in the brain. Mushroom-type spines, which have large heads and are enriched with PSD95[19], are thought to contain strong, mature synapses, while thin-type spines are more labile (Fig. 2a)[20]. The OFC is functionally and anatomically heterogenous, including along the anterior-posterior axis[2,13,21,22]. Thus, we measured spine densities in the anterior vs. posterior VLO (aVLO, pVLO). EB mice had lower densities of mushroom-type spines in the aVLO (Fig. 2b-d; $t_{(8)} = 2.286$, $p = 0.05$) and lower ratios of mushroom- to thin-type spines (Fig. 2e; $t_{(8)} = 3.104$, $p = 0.015$), consistent with PSD95 loss. We found no differences in thin- (Fig. 2d; $t_{(8)} = 0.629$, $p = 0.547$), or stubby-type spine densities (Fig. 2d; $t_{(8)} = 0.175$, $p = 0.917$). Groups did not differ in measures collected from the pVLO (Fig. 2f-h; mushroom-type $t_{(8)} = 0.454$, $p = 0.662$; thin-type $t_{(8)} = 1.539$, $p = 0.163$; stubby-type $t_{(8)} = 0.930$, $p = 0.379$; Fig. 2i; ratio of mushroom- to thin-type spines $t_{(8)} = 1.003$, $p = 0.345$).

As a comparator, we included another frontal structure involved in aspects of goal-directed behaviors, specifically learning action-outcome associations, the prelimbic cortex (PL)[23]. Analyses of dendritic spines in the anterior PL (aPL; adjacent to the aVLO) revealed no differences in spine subtype densities (Fig. 2j; mushroom-type $t_{(7)} = 0.869$, $p = 0.414$; thin-type $t_{(7)} = 0.302$, $p = 0.772$; stubby-type $t_{(7)} = 0.843$, $p = 0.427$) or mushroom- to thin-type ratio (Fig. 2k; $t_{(7)} = 0.516$, $p = 0.622$).

Synaptic marker loss in the VLO and engagement in routinized behaviors are reminiscent of features of OCD, leading to the hypothesis that EB mice would demonstrate compulsive-like behavior. We first examined amphetamine-potentiated repetitive behaviors. The premise of this test is that amphetamine will elicit repetitive behaviors like grooming and rearing, and mice prone to compulsive-like behavior will engage in these behaviors more. Groups did not differ in baseline activity following saline, and following amphetamine administration, repetitive activity increased in all mice as expected (Fig. 3a; main effect of treatment: $F_{(1,13)} = 89.65$, $p < 0.0001$). However, potentiation in EB mice was higher (interaction treatment*group: $F_{(1,13)} = 4.884$, $p = 0.046$; main effect of group: $F_{(1,13)} = 5.904$, $p = 0.030$; posthoc comparison of groups in saline condition: $t_{(13)} = 1.139$, $p = 0.275$; comparison of groups in amphetamine condition: $t_{(13)} = 2.451$, $p = 0.029$; comparison of treatments in control mice: $t_{(5)} = 3.715$, $p = 0.0138$; comparison of treatments in EB mice: $t_{(8)} = 11.62$, $p < 0.0001$). These data are also represented as difference score in activity following amphetamine relative to saline, and again, EB mice generated higher scores (Fig. 3b; $t_{(13)} = 2.212$, $p = 0.046$).

Next, separate, drug-naïve EB mice were sprayed with water, placed in a novel environment, and grooming was quantified. The premise of this test is that the typical response is for mice to both groom and explore the novel environment. Meanwhile, mice exhibiting compulsive-like behavior will groom more frequently, at the expense of exploring. As in our locomotor assays, grooming did not differ between groups at baseline (Fig. S1a), and yet, it was potentiated more so in EB mice (Fig. 3c; $t_{14} = 3.617$, $p = 0.003$).

The selective serotonin reuptake inhibitor (SSRI), fluoxetine (Prozac), is a first-line treatment for OCD in humans[24]. Thus, we next treated EB mice with fluoxetine (Fig. 3d), reasoning that any compulsive-like behavior should be reversible by fluoxetine. Fluoxetine indeed ameliorated compulsive-like grooming in EB mice (Fig. 3e; interaction group*treatment: $F_{(1,31)} = 4.342$, $p = 0.046$; no main effect of group: $F_{(1,31)} = 2.125$, $p = 0.155$; no main effect of treatment: $F_{(1,31)} = 2.799$, $p = 0.104$; posthoc comparison of groups in saline condition: $t_{(15)} = 2.287$, $p = 0.037$; comparison of groups in fluoxetine condition: $t_{(16)} = 0.489$ $p = 0.632$; comparison of treatments in ctrl mice: $t_{(15)} = 0.3228$, $p = 0.751$; comparison of treatments in EB: $t_{(16)} = 2.462$, $p = 0.026$). Altogether, these patterns demonstrate that EB mice display compulsive-like behavior that is ameliorated by the SSRI, fluoxetine.

Given evidence of synaptic marker attrition in the VLO of EB mice, we next hypothesized that chemogenetically stimulating VLO neurons could ameliorate compulsive-like behavior (Fig. 3f-g). We recorded spray-elicited grooming behavior twice: in a baseline test following 2–3 stimulations and again after a week of stimulation and created a difference score. This decision was based evidence that repeated and not subthreshold manipulation of VLO neurons induces compulsive-like behavior in other contexts[6,18]. Surprisingly, Gq-DREADDs had no impact (Fig. 3h; $t_{(11)} = 0.3418$, $p = 0.370$; raw data in Fig. S1b). DREADDs were validated by visualizing the early-immediate gene c-fos, which was elevated by Gq-DREADDs (Fig. 3i-j; $t_{(9)} = 5.993$, $p < 0.001$). In contrast, chemogenetic *inhibition* of VLO neurons mitigated grooming behavior (Fig. 3k-l; $t_{(19)} = 1.817$, $p = 0.043$; raw data in Fig. S1c). To validate the DREADDs in this case, mice were given a brief swim stressor to stimulate VLO

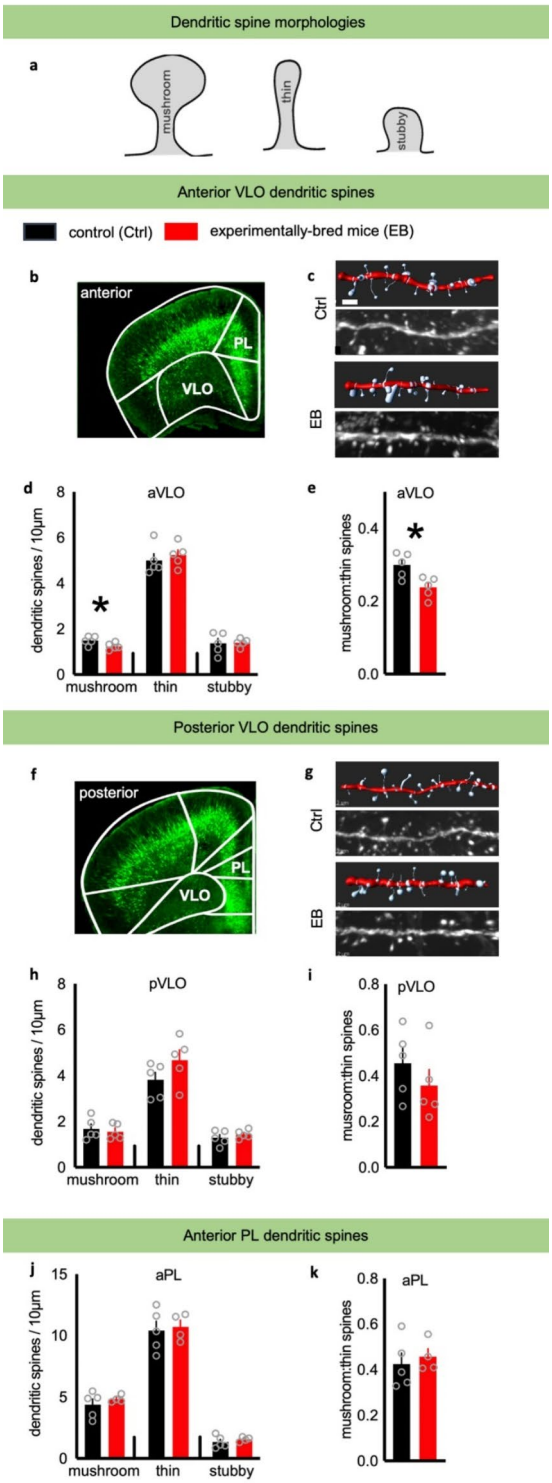

Fig. 2. Deficits in action flexibility coincide with fewer mushroom-type dendritic spines on excitatory neurons in the aVLO but not pVLO or PL. (**a**) Dendritic spine types. (**b**) Representative image of a *Thy1*-YFP-expressing coronal section from the anterior frontal cortex. (**c**) Representative aVLO dendrite reconstructions (upper) and original YFP images (lower). (**d**) The density of mushroom-type spines was lower in the aVLO of EB mice ($n = 5$/group). (**e**) Accordingly, the ratio of mushroom: thin-type spine also dropped in EB mice. (**f**) Representative image of a *Thy1*-YFP-expressing coronal section from the posterior frontal cortex. (**g**) Representative pVLO dendrite reconstructions (upper) and original YFP images (lower). (**h**) Dendritic spine type densities did not differ between groups in the pVLO. (**i**) Accordingly, the ratio of mushroom: thin-type spines also did not differ between groups. (**j**) Dendritic spine densities did not differ in the anterior PL between groups (ctrl $n = 5$, EB $n = 4$). (**k**) Accordingly, the ratio of mushroom: thin-type spines was also unaffected. Data shown as mean + SEM with circles representing individual mice. Scale bar = 2 µm. $^*p \leq 0.05$.

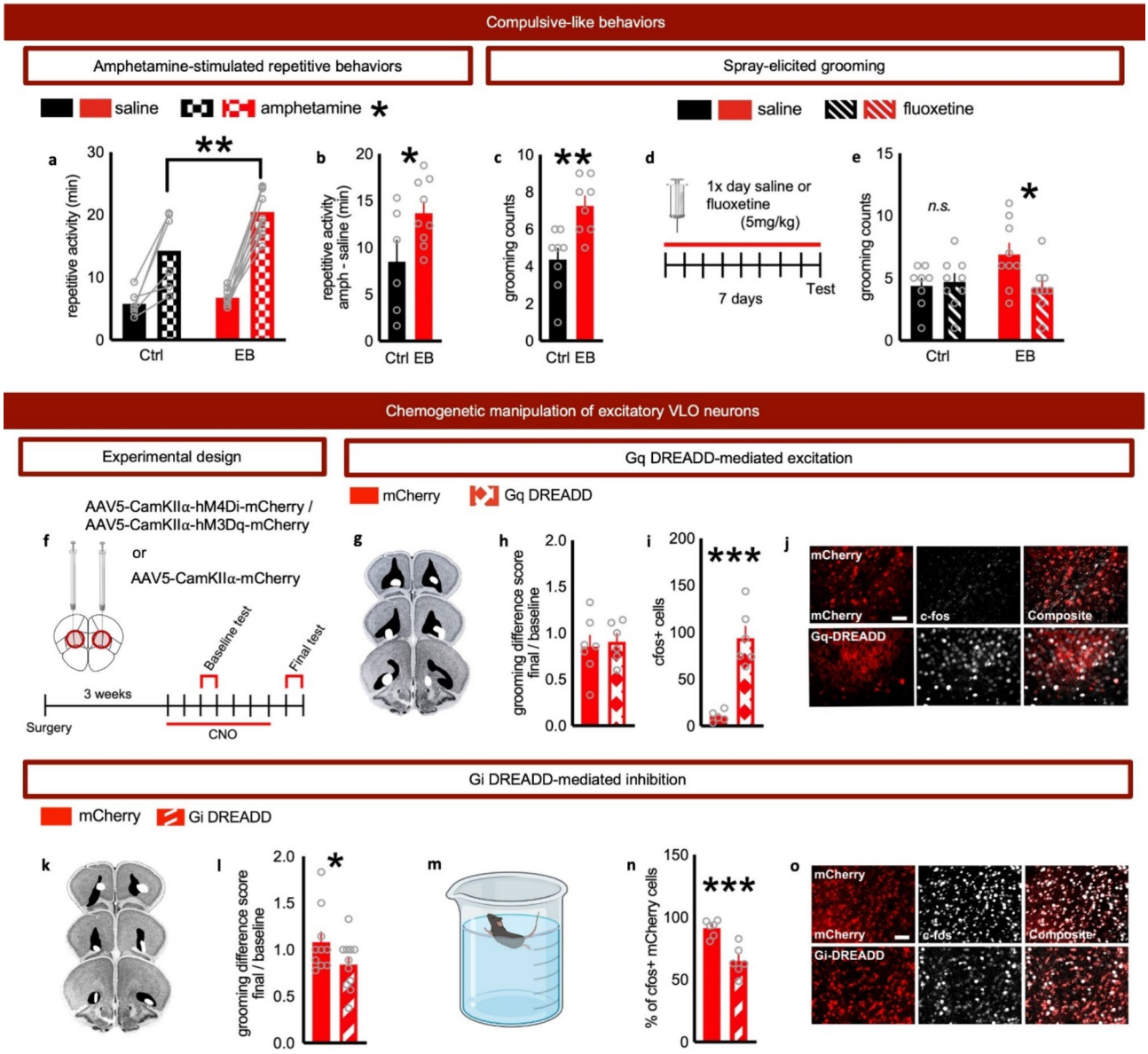

Fig. 3. Breeding mice for poor action flexibility results in compulsive-like behavior: Reversal by fluoxetine and inhibitory chemogenetics. (**a**) EB mice spent more time in repetitive behavior following amphetamine than control mice (ctrl $n = 6$, EB $n = 9$). (**b**) The same amphetamine-elicited repetitive behaviors are represented as difference score from saline baseline; again, EB mice generated more repetitive behaviors. (**c**) EB mice groomed more than control mice in a stimulus-elicited grooming test ($n = 8$/group). (**d**) Experimental schematic and timeline. (**e**) Fluoxetine ameliorated stimulus-elicited grooming behavior in EB mice (ctrl saline $n = 8$, all other groups $n = 9$). (**f**) Experimental schematic and timeline. (**g**) Histological representation of Gq-DREADDs-expressing viral vectors in the VLO is depicted on images from *The Mouse Brain Library*[63]. Black indicates the largest spread, and white the smallest. (**h**) Chemogenetic stimulation of excitatory VLO neurons had no impact on stimulus-elicited grooming, (**i**) though it did elicit c-fos at the infusion site (ctrl $n = 7$, Gq-DREADD $n = 6$). (**j**) Representative images. (**k**) Histological representation of Gi-DREADDs-expressing viral vectors is depicted on images from *The Mouse Brain Library*[63]. Black indicates the largest spread, and white the smallest. (**l**) Chemogenetic inhibition of excitatory VLO neurons mitigated stimulus-elicited grooming (ctrl $n = 10$, Gi-DREADD $n = 11$). (**m**) To validate Gi-DREADDs, mice received a swim stressor (Created in BioRender. Allen, A. (2024) BioRender.com/g86t305). (**n**) Despite this stressor, Gi-DREADDs-expressing cells displayed less c-fos, as expected. (**o**) Representative images. Data shown as mean + SEM with symbols representing individual mice. Scale bar = 50 µm. $^{*}p \leq 0.05$, $^{**}p \leq 0.01$, $^{***}p \leq 0.001$.

neurons and give us the resolution to confirm that Gi-DREADDs *decreased* c-fos levels, as expected (Fig. 3m-o; $t_{(10)} = 4.753$, $p < 0.001$).

Breeding mice for poor action flexibility and compulsive-like behavior results in changes in inhibitory synapse-associated protein levels in the VLO

The discovery that chemogenetically silencing VLO neurons ameliorated compulsive-like behavior, despite PSD95 and dendritic spine attrition, raised the possibility that proteins associated with inhibitory plasticity may also differ between EB mice and control mice. The ability to execute goal-directed behaviors is reliant on GABAergic tone in the VLO[9], so we first examined GAD67, the rate-limiting enzyme in GABA synthesis. Mice deficient in GAD67 also display compulsive-like grooming[25]. However, immunofluorescent analysis revealed *increased* levels in the aVLO of EB mice (Fig. 4a-b; $t_{(18)} = 3.021$, $p = 0.007$), which were not found in the adjacent aMO (Fig. 4c; $t_{(18)} = 1.226$, $p = 0.236$). An increase in GAD67 could reflect enhanced GABA synthesis, so this discovery led us to next examine a marker of inhibitory synapses, SLIT- and NTRK-like family member 3 (SLITRK3). Despite elevated GAD67, SLITRK3 levels were reduced in the aVLO of EB mice (Fig. 4d; $t_{(19)} = 3.305$, $p = 0.004$), a pattern that would predict fewer inhibitory synapses. Again, we found no differences in the aMO (Fig. 4e; $t_{(19)} = 1.052$, $p = 0.306$).

Within posterior regions, GAD67 levels were again higher in EB mice (pVLO; Fig. 4f-g; $t_{(18)} = 2.245$, $p = 0.0376$; pMO; Fig. 4h; $t_{(16)} = 2.147$, $p = 0.0474$), while SLITRK3 levels did not differ in the pVLO (Fig. 4i; $t_{(19)} = 1.266$, $p = 0.221$) or pMO (Fig. 4j; $t_{(19)} = 1.401$, $p = 0.177$). Thus, GAD67 levels appear to be broadly elevated in EB mice, with concurrent loss of an inhibitory synapse marker in the aVLO.

Breeding mice for poor action flexibility and compulsive-like behavior results in changes excitatory synapse-associated protein levels in the striatum

Action flexibility and compulsive-like behavior alike are coordinated through excitatory OFC connections with the striatum, where excitatory synapse markers striatin and SAPAP3 are quite enriched[26,27], so we next examined their levels (Fig. 5a). In the nucleus accumbens (NAc, also referred to as the ventral striatum), striatin levels in the shell subregion nearly differed between groups (Fig. 5b; $t_{(20)} = 1.813$, $p = 0.0848$), and were significantly elevated in the core subregion of EB mice (Fig. 5c; $t_{(20)} = 2.704$, $p = 0.014$), a pattern that would be associated with *greater* glutamatergic input. SAPAP3 protein levels did not differ in the NAc shell (Fig. 5d; $t_{(20)} = 0.709$, $p = 0.487$) or core (Fig. 5e; $t_{(20)} = 1.370$, $p = 0.186$). We found no group differences in striatin in the dorsomedial striatum (DMS) (Fig. 5f; $t_{(19)} = 0.586$, $p = 0.565$), or dorsolateral striatum (DLS) (Fig. 5g; $t_{(20)} = 0.888$, $p = 0.385$), but EB mice have lower levels of SAPAP3 in both the DMS (Fig. 5h; $t_{(20)} = 2.299$, $p = 0.032$) and DLS (Fig. 5i; $t_{(20)} = 2.086$, $p = 0.05$), a pattern that would be associated with *fewer* postsynaptic compartments receiving glutamatergic input in the dorsal striatum. Protein changes are summarized in Table 1.

In summary, mice bred to display inflexible and compulsive-like behavior suffer changes in both excitatory and inhibitory synaptic markers in the VLO. Meanwhile, protein measurements in the striatum imply that the dorsal striatum suffers a loss of glutamatergic input, while the NAc has more. Interestingly, our findings were largely localized to the aVLO. Connections between the anterior vs. posterior OFC and NAc are not, to our knowledge, yet well-characterized in the mouse. To conclude, we placed retrograde-expressing viral vectors in the NAc core (Fig. 6a) and measured the density of labeled cells along the anterior-posterior axis in the VLO and MO. Within the VLO, the highest density of labeled cells was in anterior regions, where we also observed the most consistent neurobiological effects in EB mice. Cell density declined in a step-wise fashion in more posterior regions (Fig. 6b; $F_{(1.157,\ 6.067)} = 16.46$, $p = 0.005$). In the neighboring MO, high density cell labeling was observed throughout the central MO, with fewer cells labeled in the furthest anterior and posterior segments (Fig. 6c; $F_{(2.124,\ 8.496)} = 10.34$, $p = 0.0049$). Exact post-hoc values are reported in Fig. S2.

Discussion

When familiar actions fail to produce anticipated outcomes, we often update our actions to successfully pursue rewards. Naturally, the ability to do varies from individual to individual. Here we bred mice that perform poorly in such a scenario, instead preferring routinized behaviors that are insensitive to new reward information. We first confirmed that, as previously reported[14], the offspring of these mice – termed EB (experimentally bred) mice – exhibit similar deficits as their parents. They were also unable to incorporate new information into familiar action strategies in a Pavlovian-to-instrumental transfer task. These mice provided a tool by which to investigate the degree to which inflexible action strategies are linked to compulsive-like behavior and to investigate neurobiological correlates.

Loss of action flexibility coincides with synaptic marker loss in the aVLO

In our initial behavioral experiments, mice were trained to nose poke for food reinforcers, then asked to interleave new information into their established routines – that one response is no longer rewarded in our test of action flexibility or that a cue is associated with food delivery in the Pavlovian-to-instrumental task. Mice typically inhibit a non-rewarded behavior in the first scenario, and energize food-reinforced responding in the second. In both cases, though, EB mice failed to update their behavior, insensitive to new information. The excitatory synapse marker PSD95 was reduced in the VLO of these EB mice, consistent with evidence that action flexibility in both tasks requires the VLO[2,28], and that the VLO is necessary for updating instrumental associations in general[29–31]. PSD95 loss was accompanied by attrition of mature dendritic spines on excitatory neurons and concurrent shift in the ratio of mature- to immature-type spine types. This pattern is consistent with the loss of mature spines in the most profoundly impaired EB mice in our prior report[14]. Interestingly, spine loss was contained within the aVLO, relative to pVLO and neighboring PL.

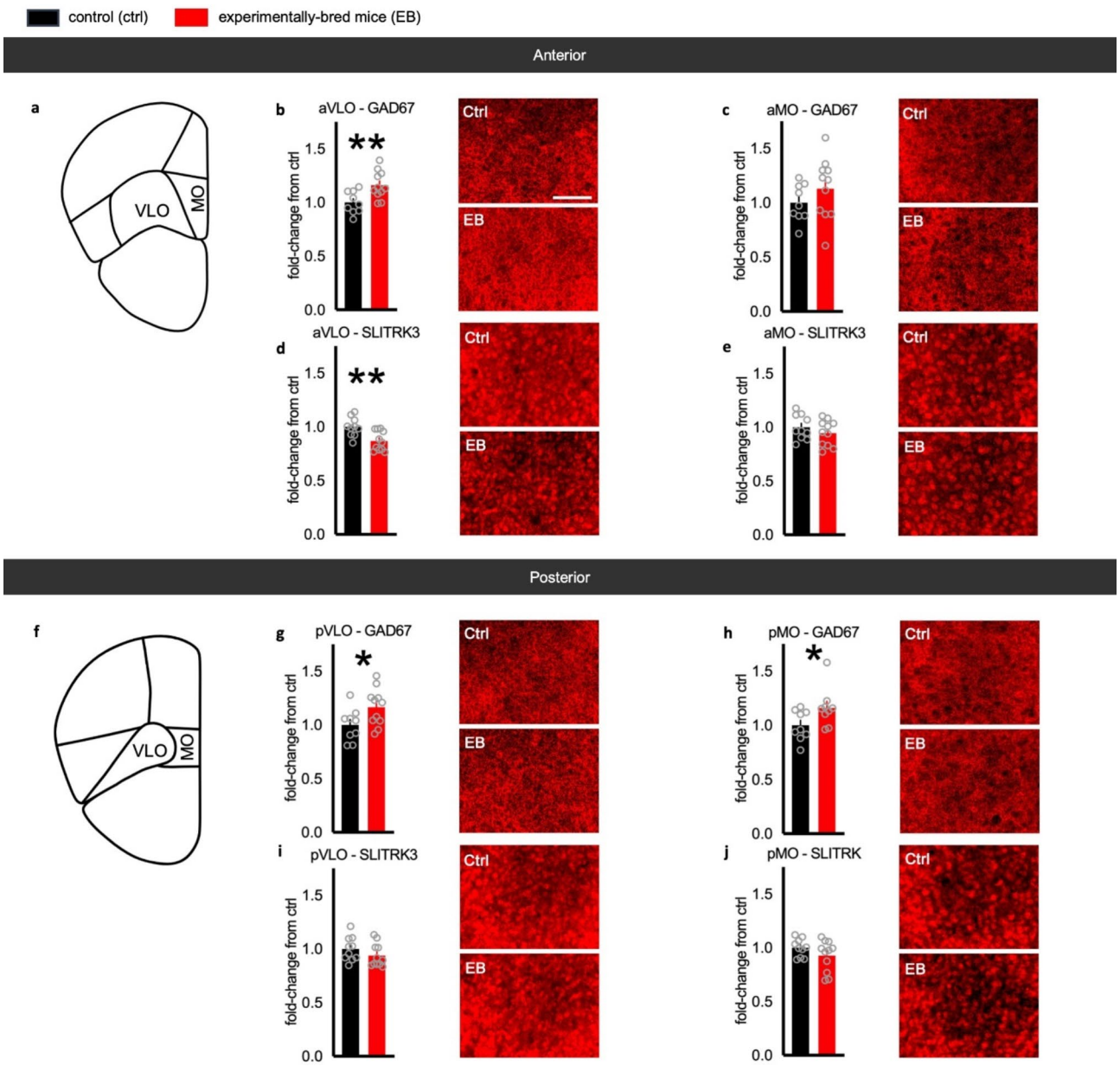

Fig. 4. Breeding mice for poor action flexibility and compulsive-like behavior results in changes in inhibitory synapse-associated protein levels in the VLO. (**a**) Coronal atlas image depicting the neuroanatomical location of the aMO and aVLO. (**b**) EB mice had higher levels of GAD67 in the aVLO. (**c**) GAD67 levels in aMO. did not differ between groups. (**d**) Meanwhile, in the aVLO, SLITRK3 was lower. (**e**) SLITRK3 levels did not differ in the aMO. (**f**) Coronal atlas image depicting the neuroanatomical location of the pMO and pVLO. (**g**) GAD67 levels were higher in the pVLO of EB mice and (**h**) in the pMO. (**i**) SLITRK3 levels did not differ between groups in the pVLO or (**j**) pMO. Ctrl refers to same-strain age-matched mice. Data shown as fold-change from control mean + SEM with circles representing individual mice. Ctrl $n = 9–10$, EB $n = 9–11$, with representative immunofluorescent images inset. Scale bar = 50 µm. $^{*}p \leq 0.05$, $^{**}p < 0.01$.

How could these changes contribute to action inflexibilities? In nonhuman primates trained to respond for food reinforcers, pVLO inactivation rendered them unable to respond to changes in food values, consistent with long-appreciated function of the OFC in value processing. Meanwhile, aVLO inactivation caused failures in value memory retrieval[32]. In other words, *after* outcome values were updated, the aVLO was necessary for the recall of that information for organisms to direct their future choices appropriately. Similarly, the aVLO in rodents is necessary for action strategy updating, its function including retrieval of new action memories[2,8]. Potentially, the aVLO supports action flexibility by retrieving memories of strategies that have been effective or ineffective in the past.

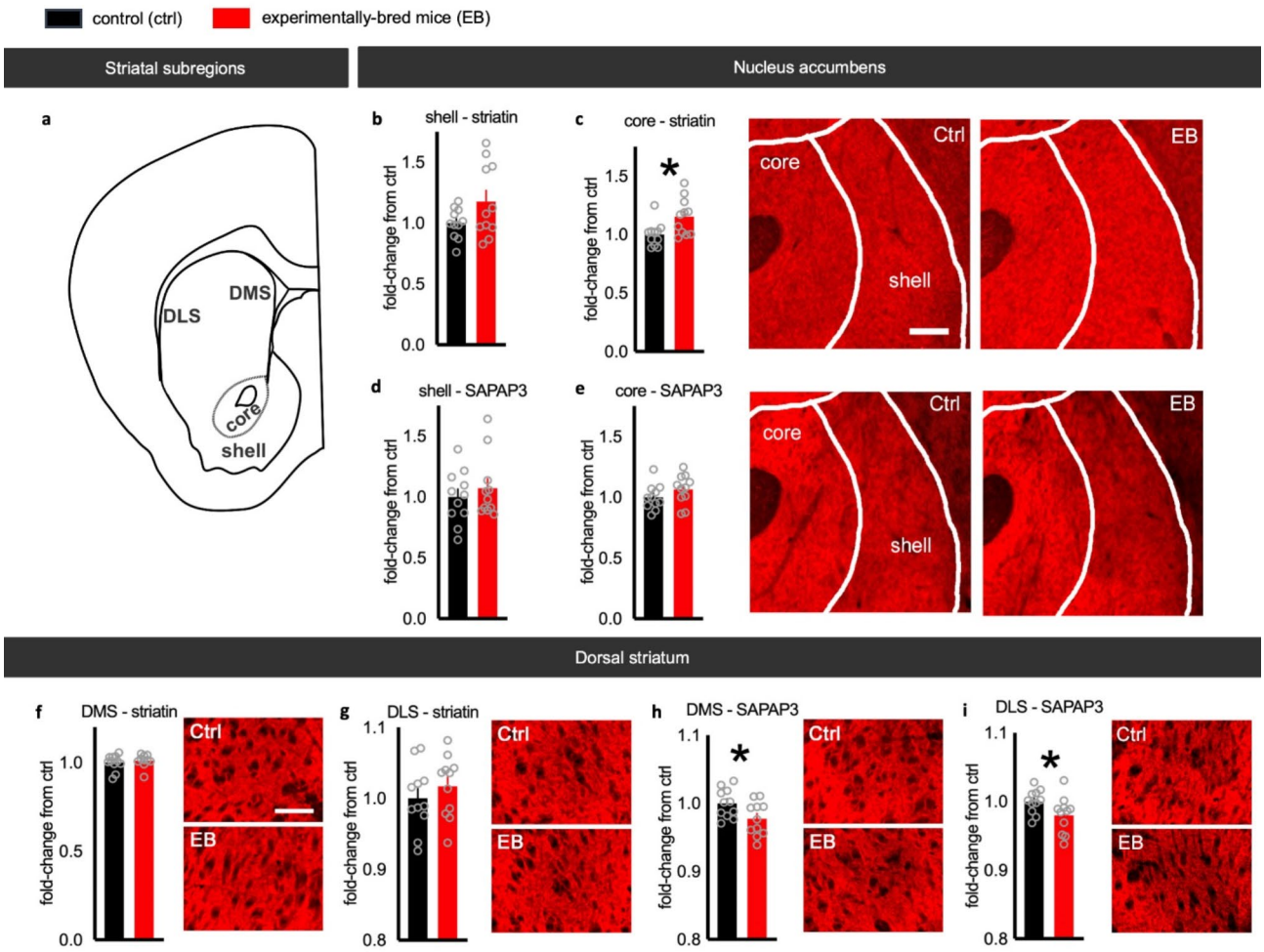

Fig. 5. Breeding mice for poor action flexibility and compulsive-like behavior results in changes excitatory synapse-associated protein levels in the striatum. (**a**) Coronal atlas image depicting the neuroanatomical location of the DMS, DLS, NAc shell, and NAc core. (**b**) Striatin levels in the NAc shell do not differ between groups ($n = 11$/group), but (**c**) differed in the NAc core. (**d**,**e**) SAPAP3 levels in NAc did not differ between groups. (**f**,**g**) Striatin levels in the DMS and DLS did not differ between groups. (**h**,**i**) SAPAP3 levels in the DMS and DLS are lower in EB mice. Data shown as fold-change from control mean + SEM with circles representing individual mice. Representative immunofluorescent images inset. Scale bars = 200 µm. $^*p \leq 0.05$.

Protein	aVLO	pVLO	aMO	pMO
GAD67	↑↑	↑	n.s.	↑
SLITRK3	↓↓	n.s.	n.s.	n.s.
Protein	**DMS**	**DLS**	**NAc core**	**NAc shell**
Striatin	n.s.	n.s.	↑	n.s.
SAPAP3	↓	↓	n.s.	n.s.

Table 1. Summary of immunofluorescent protein quantification experiments. ↑ and ↓ refer to $p \leq 0.05$, ↑↑ and ↓↓ refer to $p \leq 0.01$. *n.s.* refers to non-significant.

Mice bred to demonstrate action inflexibility also demonstrate compulsive-like behavior

Action inflexibility in EB mice resembles habitual behavior, which is insensitive to changes in action-outcome contingency[33]. And in a prior investigation, we indeed confirmed that EB mice are biased towards habitual behaviors in classical assays[18]. Habits are often considered antecedent to compulsion[15,34], which led us to next question whether EB mice display repetitive, compulsive-like behavior. In a model of repetitive behavior, a single exposure to amphetamine indeed elicited repetitive behaviors to a greater degree in EB than control mice. And in a spray-elicited grooming test, EB mice spent more time grooming, indicative of compulsive-like behavior.

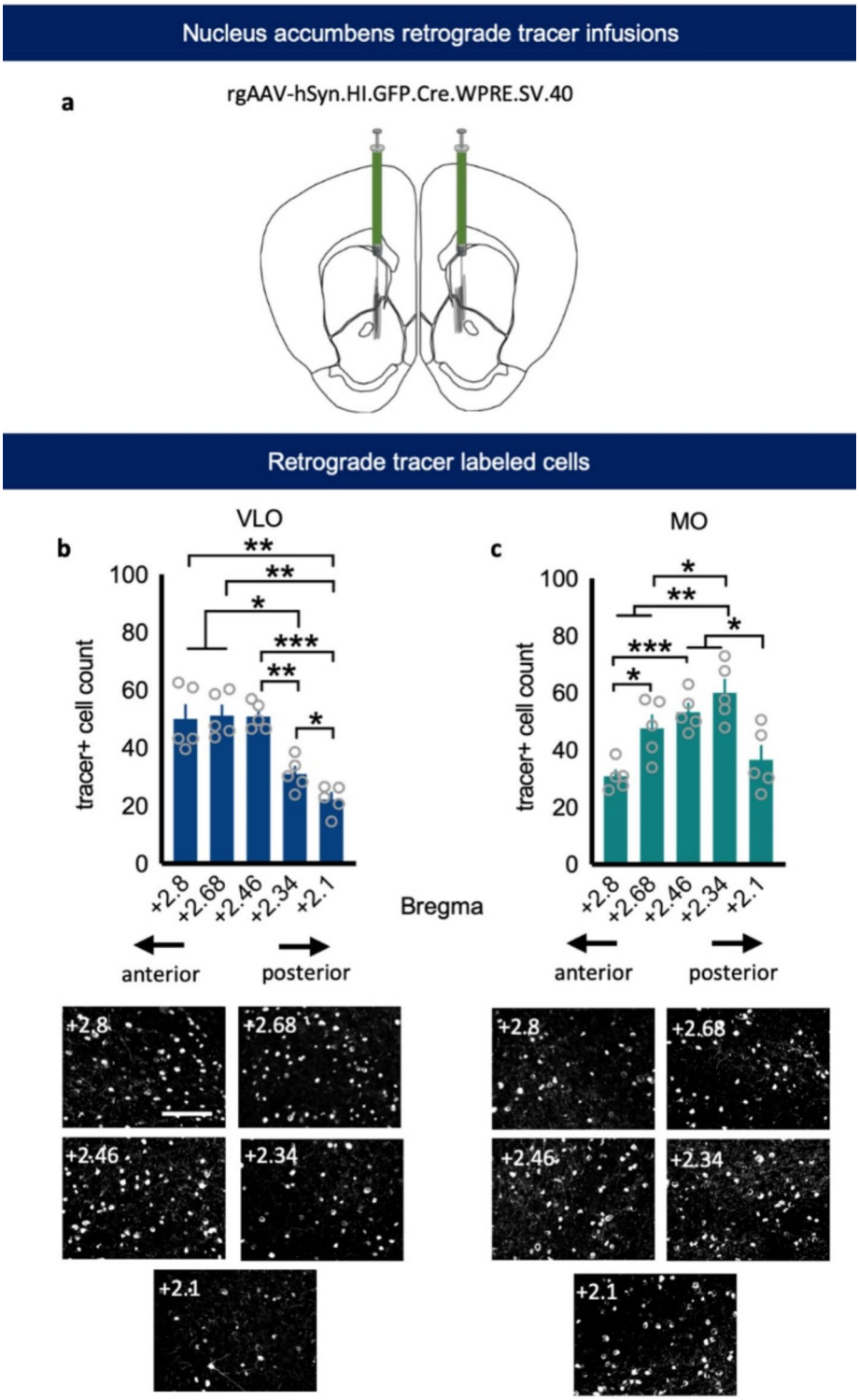

Fig. 6. Orbito-striatal projection patterns differ along the anterior-poster axes. (**a**) Coronal atlas image depicting bilateral retrograde tracer infusion sites in the NAc. Tracer labeled cell bodies were quantified in the VLO and MO ($n = 5$). (**b**) The anterior VLO had more labeled cells than the posterior. (**c**) The central MO contained more tracer labeled cells than the anterior- or posterior-most regions. Data shown as mean number of tracer-positive cells per field + SEM, with circles representing individual mice. Representative immunofluorescent images below. Scale bars = 100 µm. $^{*}p \leq 0.05$, $^{***}p \leq 0.001$.

Spray-elicited grooming was ameliorated by fluoxetine, a first-line treatment for OCD, lending the model predictive validity.

Excitatory dendritic spine attrition in EB mice was reminiscent of excitatory synapse marker loss in humans with OCD[11] and evidence that optogenetic stimulation of excitatory OFC neurons can ameliorate compulsive-like behavior in genetic models for studying compulsion[35]. Thus, we thought it logical to test whether chemogenetic stimulation of excitatory VLO neurons could ameliorate compulsive-like grooming. However, we observed no evidence for this, and instead, chemogenetically *silencing* excitatory VLO neurons normalized grooming behavior. These findings were somewhat surprising. On the other hand, one of the most consistent findings in humans with OCD is hyper-activity within the OFC[36], and in mice, stimulating excitatory VLO neurons – particularly those positioned in the more medial zones of the VLO and in the MO itself – can induce compulsive-like behavior[6,18]. These effects appear to be attributable to select cell populations expressing melanocortin receptors[18] and/or projecting to the NAc[6].

The unexpected combination of spine loss and amelioration of behavioral phenotypes by inhibitory chemogenetic led us to next consider factors related to inhibitory neurotransmission. GAD67, the rate-limiting enzyme in GABA synthesis, was elevated in the aVLO, pVLO, and even adjacent pMO of EB mice, pointing to a potential broad spread upregulation of GABA synthesis[37,38]. This discovery is consistent with evidence that in mutant mouse models for studying compulsion, inhibitory neural activity in the OFC is *elevated* during bouts of grooming, which is normalized by fluoxetine[39]. And yet, SLITRK3, a post-synaptic protein necessary for inhibitory synapse development[40], declined in the aVLO, consistent with inhibitory synapse attrition[40]. Altogether, the neurobiological consequences of experimental breeding point to broad spread elevated GABA synthesis and to the aVLO as site suffering from loss of both excitatory and inhibitory inputs in EB mice. Optimal neuron function is dependent on the summation of excitatory and inhibitory signal transduction[41]. These alterations could impact the ability of neurons to optimally process incoming projections necessary for action flexibility, for instance from the basolateral amygdala[2,42,43], and to effectively convey signals to downstream structures involved in instrumental action and compulsive-like behavior.

Mice bred to demonstrate action inflexibility and compulsive-like behavior suffer changes in excitatory synapse markers in the striatum

Finally, we measured striatin and SAPAP3 in the dorsal striatum and NAc. Striatin and SAPAP3 are postsynaptic markers of excitatory synapses highly enriched in the striatum[27,44]. Specifically, striatin is highly expressed in dendritic spines receiving glutamatergic inputs[26,45], while SAPAP3 is localized to the postsynaptic density of glutamatergic synapses[27]. Action flexibility and compulsive-like behaviors alike are controlled by excitatory OFC connections with striatal output structures[15,17]. Further, genetic variants in *DLGAP3*, the gene encoding SAPAP3, are associated with OCD, and individuals with OCD have lower striatal *DLGAP3* expression[11]. *Sapap3*$^{-/-}$ mice exhibit compulsive-like behavior, which is alleviated by: the SSRI fluoxetine[46]; restoring SAPAP3 expression in the dorsal striatum[46]; and stimulating VLO-to-dorsostriatal neurons[35]. And finally, compulsive-like behavior in mice can be *induced* via stimulation of OFC-to-NAc neurons[6], altogether suggesting that imbalance cortio-striatal connections could drive compulsive-like behavior. Consistent with this model, EB mice had less SAPAP3 in both the DMS and DLS. Meanwhile, striatin levels were higher in the NAc. Together, this pattern points to the possible attrition of excitatory contacts in the dorsal striatum and elevated synaptic strength or number of synapses from glutamatergic projections into the NAc.

As noted, our findings converged on the aVLO as a site where EB mice regularly differed from control counterparts. Connections between the anterior vs. posterior VLO and NAc are not, to our knowledge, conclusively mapped, particularly relative to those between the VLO and dorsal striatum. Thus, we lastly used retrogradely acting viral vectors infused into the NAc to determine whether the aVLO projects to the NAc in mice. Within the VLO, projections spanned the anterior-posterior axis, with most robust densities in the anterior sections, at a plane where VLO-to-striatum projections have also been documented in rats[47]. The MO also innervated the NAc, also as in rats[48]. For instance, Bradfield and colleagues documented MO-to-NAc connections across the anterior-posterior axes, revealing dense projections from what was codified as anterior MO in their study[13], and that corresponds with the mid-point in our analysis here. Further, very posterior OFC regions (beyond those examined here) appear to innervate the NAc[49,50]. Not captured in our dataset is evidence that while VLO-to-NAc projections have been documented, they are modest relative to dorsal striatum projections, and they derive from the more lateral VLO areas, while the more medial section preferentially innervates the dorsal striatum over NAc[47,48,51,52]. Orbito-striatal projections terminate on both dopamine D1 and D2 receptor-containing medium spiny neurons, the primary neuron subtypes in the striatum[53]. Extensive connectivity with the striatum likely endows the OFC with enormous capacity to modulate reward-seeking and compulsive-like behaviors.

Conclusions

Here we discovered that mice bred to favor habit-like behaviors also display compulsive-like behavior. Importantly, though, we are not equating habitual and compulsive-like behavior. Compulsion often involves intense focus and desire to complete an act (like handwashing, for instance) – antithetical to habitual behavior. A shared feature, though, is repetition, and often, behaviors are triggered by environmental events, which was the case with EB mice here. Specifically, these mice do not demonstrate repetitive motor behaviors at rest, but amphetamine and water spray unleashed repetitive actions. These behaviors were associated with several neurobiological modifications in cortico-striatal structures and ameliorated by repeated chemogenetic silencing of excitatory VLO neurons. In related reports[6,18], cells in the VLO were repeatedly stimulated to *induce* compulsive-like behavior, while acute manipulation was without consequence. Conceivably, behavioral effects are attributable to slow-acting neurosequelae. For instance, if dendritic spine and synaptic marker loss was a consequence of

excitatory: inhibitory imbalance here, one can imagine that repeated intervention might be required to correct a constellation of outcomes occurring at the levels of neuronal architecture, synaptic contacts, and protein content.

One might ask, are the same mechanisms responsible for action inflexibility in these EB mice, or do compulsive-like behaviors derive from distinct biological changes? Insights could be gained by discerning what induces transgenerational deficits in response flexibility in the first place. Genetic variation seems unlikely, given the rapidity by which the phenotype emerged (within a couple of generations). Another approach would be to isolate the VLO cell populations that control compulsive-like grooming relative to reward-seeking action strategies[39]. Mapping and manipulating their striatal connectivity could reveal mechanisms (shared or distinct) by which each controls respective behaviors.

Methods

Subjects

Experimentally bred (EB) mice were originally described in Allen et al., 2022[14] and maintained on a C57BL/6J background. They express *Thy1*-driven Yellow Fluorescent Protein (YFP) (H line[54]) to facilitate visualization and reconstruction of neuronal dendritic spines. Throughout, age- and strain-matched YFP-expressing mice on a C57BL/6J background that were bred in-house were used as control mice. Original breeding pairs were sourced from Jackson Labs. Mice were maintained on a 12 h. light cycle (0700 on) with food and water provided ad libitum except during behavioral testing when food was restricted to motivate responding for food reinforcers. Mice were tested during the light cycle except for when locomotion was monitored over 24 h.

Upon weaning at ~postnatal day (P) 21, mice were housed in single-sex cages. Mice screened for later breeding (described immediately below) began behavioral testing at P27-30. Other procedures occurred at or soon after P56. Both sexes were used except for tracing experiments, which used males. Sex composition is reported in Table S1. Sex ratio was at times imperfectly balanced due to the availability of EB mice and same-age, same-strain controls. We did not detect trends that would point to sex differences.

Studies were performance in accordance with ARRIVE guidelines. Experiments and procedures were approved by the Emory University IACUC (protocol #201700227) and conducted in compliance with the Emory University IACUC guideline (protocol #201700227). Emory University is an AAALAC accredited institution.

Method to identify mice for experimental breeding

To motivate food-reinforced responding, young mice were food restricted such that they gained only enough weight to match Jackson Labs growth curves for C57BL/6 mice. Operant conditioning chambers (Med-Associates) were equipped with 3 nose poke ports, and a separate food magazine. During training, responding on 2 ports was reinforced with food pellets (20 mg, Bio-serv) on a fixed ratio 1 (FR1) schedule. Training sessions ended after 60 pellets were delivered (30 on each port) or timed out after 70 min., and occurred once per day for 7 days. Mice did not display side preferences, and response acquisition curves represent responses on both ports per min.

Next, 1 of the 2 previously active ports was physically occluded while the response-outcome relationship remained intact on the available port, meaning, responses resulted in pellet delivery. The following day, the previously available port was occluded, and the previously occluded port was available. Now, responses on this port had no programed outcome. Instead, pellets were delivered independently from responses and at a rate matching that of the previous session. Thus, the established response-outcome relationship associated with this port was violated. This 2-day procedure was conducted twice, and each session was 25 min. The location of the "non-reinforced" port within the chamber and the order in which these sessions occurred were counterbalanced. Finally, mice were tested to see if they preferred the "reinforced" nose poke in a probe test. During this 10-min. session, all ports were available, and responding was not reinforced.

Following behavioral testing, mice were left undisturbed until P56 or older. Mice were then paired for breeding if they had fulfilled 2/3 of the following criteria when tested in the above-described task: *1)* > 20% of total responses occurred on the inactive port during response training; *2)* they failed to inhibit responding during the initial "non-reinforced" session relative to "reinforced" session; or *3)* they failed to prefer the "reinforced" nose poke during a choice test that was conducted the day after the procedure described above. During this 10-min. session, all ports were available, and responding was not reinforced. To maintain the line, every generation of breeding mice was behaviorally tested, and mice were selected for breeding based on these criteria. Mice used for other behavioral tests were not subject to this screening.

Test of action flexibility in the offspring of experimentally bred mice (Fig. 1)

The establishment of this line of mice was first reported in Allen et al., 2022[14]. The offspring of EB mice (referred to here as EB mice) and their same-age matched control counterparts were randomly assigned sequential identifiers upon weaning (i.e., 0, 1, 2, 3), and then all mice in a given litter were trained and tested. In our initial report[14], the first mouse of each sex from each litter was selected, and their response rates were reported. In this manuscript, the last mouse of each sex from each litter was selected for re-confirmation of response biases in the offspring of EB mice. If both sexes were not available, then 2 mice of the same sex were included. No more than 2 mice/litter were included in analyses to avoid litter effects. This task is the same as that used to identify mice for experimental breeding, described above, except that the choice test was omitted.

Pavlovian-to-instrumental transfer

Pavlovian-to-instrumental transfer (PIT) was conducted as previously described[42] in operant conditioning chambers containing 2 nose poke ports with recessed lights, a retractable lever, a separate food magazine, and a house light (Med-Associates). To motivate food-reinforced responding, mice were food restricted until reaching ~93% of their free-feeding weight. Mice were otherwise behaviorally naïve.

Pavlovian conditioning
The 2 nose poke port lights served as the conditioned stimuli (CS) during Pavlovian conditioning. In 30 min. sessions, 1 of 2 nose poke port lights was illuminated; one serving as the CS+, during which food pellets were delivered every 30 s., and the other serving as the CS-, during which no pellets were delivered. Each mouse underwent both conditions daily, the order of which were randomized across days, and magazine entries were recorded. Sixteen sessions were conducted.

Instrumental conditioning
Instrumental conditioning followed Pavlovian conditioning. In the same conditioning chambers, the house light was illuminated, CS + and CS- lights extinguished, and the retracted lever was extended. In 30 min. sessions conducted once per day for 4 days, lever pressing (active responding) was reinforced on an FR1 schedule, while entries on the nose poke ports (inactive responding) were recorded but had no programmed outcome.

Transfer test
Finally, the transfer test occurred. It was conducted in the same conditioning chambers in extinction. The house light was illuminated, the lever extended, and the CS + and CS- were presented 3x in alternating 30 s. intervals over the 6 min. session. Response rates during the CS + and CS- conditions were compared.

Amphetamine-elicited repetitive behaviors

Mice received *i.p.* injections of saline once daily for 3 days prior to testing to habituate them to injection stress. Each mouse then underwent 2 test sessions, 72 h. apart, conducted under dim light. Locomotor monitoring chambers (17 in. x 1.5 in. x 8.25 in.) were equipped with 16 photobeams (Med-Associates). Mice were habituated to the testing room for 1 h. before receiving an injection of amphetamine (3 mg/kg in saline at 1 mL/100 g, *i.p.*; Sigma) or saline and being placed in photobeam-equipped chambers for the 1 h. session. Mice were tested in the opposite condition in the other session; the order of saline vs. amphetamine injection was counter-balanced. Time spent repeatedly interrupting individual photobeams, as would occur during rearing or grooming, was quantified and reported as repetitive activity.

Ambulatory activity

Ambulatory activity was recorded for 24 h. using the same locomotor monitoring system as above. Mice were placed individually in large, clean arenas with bedding materials at the start of the test. Ambulatory activity was quantified as sequential photobeam breaks across the 24 h. period in 1 h. bins. Mice were not habituated to the chambers or room beforehand.

Surgery

Mice were anesthetized with ketamine (100 mg/kg, *i.p.*) and dexmedetomidine (0.5 mg/kg, *i.p.*) administered at 1 mL/100 g and placed in a digitized stereotaxic frame (Stoelting). Surgeries were performed under aseptic conditions. A mid-sagittal incision exposed the skull, and a craniotomy was performed to allow for intracranial viral vector infusion. aVLO infusion volumes and coordinates relative to Bregma were 0.5 µL per hemisphere at ML: ±1.20 mm, AP: +2.60 mm, DV: -2.80 mm. Mice were randomly assigned to receive either the inhibitory chemogenetic receptor (AAV5-CamKIIα-hM4Di-mCherry, 2.4×10^{12} GC/mL, Addgene #50477, deposited by Bryan Roth), the excitatory chemogenetic receptor (AAV5- CamKIIα-hM3Dq-mCherry,1.7×10^{13} GC/mL, Addgene #50476, deposited by Bryan Roth), or a control construct (AAV5-CamKIIα-mCherry, 4.9×10^{12} GC/mL, UNC GTC Vector Core #AV4809E, deposited by Karl Deisseroth), which was infused bilaterally. NAc infusion volumes and coordinates relative to Bregma were 0.5 µl per hemisphere at ML: ±0.95 mm, AP: +1.5 mm, DV: -4.2 mm. The retrograde fluorescent construct (rgAAV2-hSyn.HI.GFP.Cre.WPRE.SV.40, 7×10^{12} GC/mL, Addgene #105540, deposited by James M. Wilson) was infused bilaterally. Half of the mice that received retrograde tracer infusions had received cocaine (10 mg/kg in saline, *i.p.*, daily for 5 days, with the other half receiving saline only) 2 weeks prior to being euthanized for an unrelated experiment; cocaine status did not impact cell body counts. Infusions occurred over the course of 5 min. using a microliter syringe (Hamilton), which was left in place for an additional 5 min. before retraction to restrict off-target viral vector spread.

Stimulated grooming assay

This assay was adapted from Xu et al. (2013)[55]. The experimenter gently suspended each mouse by the tail and rapidly sprayed the mouse 6 times with clean water using a standard laboratory spray bottle positioned roughly 6 in. from the mouse's body. Mice were then immediately placed in a large clean cage (15.5 in. x 13 in. x 7.5 in.) and observed every 30 s. for a total of 12 observations (6 min. test), and instances of grooming were recorded. A mouse displaying compulsive-like behavior will groom more than control mice, at the expense of exploring the novel environment. As a control, grooming counts in the absence of spray were also collected by exactly replicating all steps of the procedure, except the trigger on the spray bottle was not depressed (thus, the mice were not sprayed).

The two tests (no spray vs. spray) were conducted on the same day, morning and afternoon, in a counter-balanced fashion. Grooming behaviors in a given experiment were scored by a single experimenter who was blind to group.

Fluoxetine

For 7 days prior to the grooming test, mice were injected once daily with fluoxetine (5 mg/kg in saline at 1 mL/100 g, *i.p.*; Sigma) or saline alone. After the final injection, mice were quietly transported from the vivarium to a testing room and allowed to habituate overnight. The stimulated grooming assay occurred the following day.

Clozapine *N*-oxide (CNO)

In grooming experiments with mice expressing chemogenetic receptors, all mice, regardless of viral vector, received daily injections of CNO (1 mg/kg in 2% DMSO in saline at 1 mL/100 g, *i.p.*; Sigma) for 7 days. A baseline grooming test was first conducted before the CNO injections on days 3 or 4. We chose this timeline based on prior publications that also established baseline grooming counts on days 3 or 4 and then revealed that compulsive-like grooming is induced by repeated stimulation of VLO neurons[6,18]. Then, after completion of the 7-day CNO regimen, the second stimulated grooming test was conducted on days 8 or 9, as depicted in figure timeline. Grooming counts and difference scores (post-CNO grooming bouts - baseline grooming bouts) are reported.

Sample preparation for validation of Gi-DREADD efficacy

Mice expressing control or Gi-DREADD-expressing viral vectors were administered CNO (1 mg/kg in 2% DMSO in saline at 1 mL/100 g, *i.p.*; Sigma) 30 min. prior to being placed in room temperature water in a 4 L beaker, placed in a sound attenuating chamber. The purpose was to induce a stress response and stimulate VLO neurons, giving us the resolution to detect a suppression of immediate-early gene expression by Gi-DREADDs. No data were recorded. After 6 min., mice were briefly patted dry with clean paper towels, and placed in a clean cage on a heating pad for 1 h. prior to being euthanized. Mice were deeply anesthetized by ketamine/xylazine (120 and 10 mg/kg, respectively, *i.p.*) until unresponsive, followed by transcardial perfusion with phosphate-buffered saline, then 4% paraformaldehyde. Brain tissues were post-fixed for 48 h. in 4% paraformaldehyde at 4 °C, then transferred to 30% w/v sucrose until sectioning to confirm infusion site placement and conduct c-fos immunofluorescent staining.

Western blotting

Behaviorally naïve mice were briefly anaesthetized by isoflurane and euthanized by decapitation. Brains were rapidly extracted and frozen at -80°. Brains were later sectioned using a chilled brain matrix and samples collected bilaterally using a 1.5 mm tissue punch. The VLO was identified based on neuroanatomical landmarks on the anterior side of the coronal section. Samples spanned the anterior-poster extent of the VLO due to the thickness of the section. Samples were sonicated in lysis buffer containing protease and phosphatase inhibitors (Cell Signaling 5872 S), and protein content was determined by BCA assay (Pierce Scientific 23225). Samples were then denatured in sample buffer containing 10% 2-Mercaptoethanol and boiled at 90° for 5 min. Sample buffer containing 15 µg of denatured protein was separated by electrophoresis using 4–20% polyacrylamide stain-free gels (BioRad 4568046) and total protein imaged.

Samples were next transferred to PVDF membranes and blocked in blocking buffer (5% w/v skim milk + 0.01% Tween-20) in tris-buffered saline (TBS; 7.4 pH) for 1 h. at room temperature. To simultaneously quantify multiple proteins, blots were cropped into segments based on molecular weight markers before being incubated with primary antibodies overnight at 4 °C. Anti-PSD-95 (Cell signaling 3450s[14], 1:1,000) and GluN1 (Millipore 05-432[56], 1:500) antibodies were diluted in blocking buffer. Following 3 washes in TBS, HRP-conjugated goat anti-rabbit secondary antibody (Cell Signaling 7074s; 1:15,000) was diluted in blocking buffer and membranes incubated for 1 h. at room temperature. After 3 washes in TBS, membranes were incubated in chemiluminescent substrate (Pierce) and imaged using a ChemiDoc MP Imaging System (BioRad). Densitometric values were individually normalized to corresponding total protein. Within each membrane, values were normalized to the mean of control values to control for variance between membranes.

Retrograde tracer imaging and quantification

Seven weeks after tracer infusion, mice were deeply anesthetized by ketamine/xylazine (120 and 10 mg/kg, respectively, *i.p.*) until unresponsive, followed by transcardial perfusion with phosphate-buffered saline, then 4% paraformaldehyde. Brain tissues were post-fixed in 4% paraformaldehyde for 24 h., followed by overnight incubations in 10%, 20% and 30% sucrose at 4 °C, before being flash frozen and stored at -80 °C. Twelve µm-thick sections were collected on a CryoStar NX70 cryostat and stored at -80 °C on Superfrost Plus Slides. Slides were then heated to 60 °C for 30 min., before being postfixed in 4% paraformaldehyde for 15 min., and dehydrated through an ethanol gradient (50%, 70%, 100%, 100% − 5 min. each). Once dry, slides were cover slipped and imaged on a Keyence BZ-X710 microscope. Images were divided into 5 levels across the anterior-posterior axis between Bregma + 2.8 and + 2.1. The "identify primary objects" function of CellProfiler[57] was used to quantify tracer + cells at each Bregma level of the VLO and MO. Each mouse contributed 3 images per Bregma level, the mean of which is reported.

Dendritic spine imaging and reconstruction

Behaviorally naïve mice were briefly anaesthetized by isoflurane and euthanized by decapitation. Brains were incubated in 4% paraformaldehyde for 48 h at 4 °C before being transferred to 30% w/v sucrose until sectioning. Fifty µm-thick coronal brain sections were collected on a Microm HM 450 freezing microtome and stored in cryoprotectant at 4 °C before being mounted on Superfrost Plus Slides and imaged. Z-stack images of layer V neurons expressing *Thy1*-driven YFP were collected on a Leica microscope with a spinning disk confocal (VisiTech International) at 100 × 1.4 numerical port objective using a 0.1 µm step size. Basilar dendrites with adequate separation from neighboring dendrites for clear dendritic spine visualization were selected. Six to 8 segments that were 20–30 µm in length per mouse were imaged from both the aVLO (Bregma + 2.8 - +2.46) and pVLO (posterior to Bregma + 2.46). Neurons in the aPL were imaged as a comparator. Imaris (Bitplane) software was used to create 3-D dendrite reconstructions using the FilamentTracer module as previously described[58,59].

All dendritic spines on a given segment were reconstructed. Spine types were identified within the VLO by the following criteria: Mushroom-type spines had a head diameter: minimum neck diameter > 1.5:1 and a head

diameter > 0.7 μm. Thin-type spines had either a head diameter: minimum neck diameter > 1.5:1 and a head diameter ≤ 0.7 μm, or a head diameter: minimum neck diameter ≤ 1.5:1 and a spine length: head diameter > 2.5:1. Within the aPL, spine types were identified as previously described[60]. Briefly, mushroom-type spines were determined by a head diameter: minimum neck diameter > 1.1:1 and head diameter > 0.4 μm. Thin-type spines had either a head diameter: minimum neck diameter > 1.1:1 and head diameter ≤ 0.4 μm, or a head diameter: minimum neck diameter < 1.1:1 and spine length: minimum neck diameter > 2.5. Stubby-type spines had a head diameter: minimum neck diameter < 1.1:1 and spine length: minimum neck diameter ≤ 2.5. Experimenters were blinded to group.

Immunofluorescence

Mice had been behaviorally tested but were drug naïve. They were deeply anesthetized by ketamine/xylazine (120 and 10 mg/kg, respectively, *i.p.*) until unresponsive, followed by transcardial perfusion with phosphate-buffered saline, then 4% paraformaldehyde. Brain tissues were post-fixed for 48 h. in 4% paraformaldehyde at 4 °C, then transferred to 30% w/v sucrose until sectioning. Fifty μm-thick coronal sections were collected using a Microm HM 450 freezing microtome and stored in cryoprotectant until histological processing. First, sections were washed in TBS to remove cryoprotectant before incubation in blocking buffer (5% normal goat serum [NGS], 0.03% Triton X-100 [Sigma X100]) for 1 h. at room temperature. Primary antibodies were GAD67 (Cell Signaling 413182; 1:5,000), SLITRK3 (Sigma SAB3500965; 1:250), SAPAP3 (Invitrogen PA5-20465; 1:5,000), striatin (Novus NB110-74571; 1:250), and c-fos (Abcam 190289; 1:1,000). Both primary and secondary antibody solutions contained 1% NGS and 0.03% Triton X-100 in TBS. Primary antibody incubation was overnight at either 4 °C (GAD67, SAPAP3, c-fos) or at room temperature (SLITRK3, striatin). Primary solutions were removed with TBS washes prior to secondary antibody incubation with either goat anti-mouse Alexa647 (Invitrogen A21235, 1:1000) or goat anti-rabbit Alexa647 (Invitrogen A32733, 1:1,000) for 1 h. at room temperature. Due to the limited number of OFC sections available, and occasional section damage, group sizes were not equal across antibodies.

Sections were mounted on Superfrost Plus Slides and z-stack images (0.8 μm step) acquired using a Keyence BZ-X710 microscope with uniform exposure parameters, which were compressed to a single best focus image, and pseudo-colored prior to analysis. Analyses of NAc shell images were preformed using ImageJ[61] software to allow for a drawn region of interest in order to exclude the NAc core region (quantified separately). Other images included only the region of interest, and were analyzed using CellProfiler software[57]. The analysis pipeline for quantification of c-fos + mCherry-expressing cells included intensity thresholding (Otsu method). All c-fos analyses included automated cell counting of c-fos objects based on the size of the object diameter. In the Gq-DREADD c-fos analysis, c-fos counts within mCherry regions are reported. In the Gi-DREADD c-fos analysis, the number of mCherry-expressing c-fos + cells is reported. This method of quantification was selected because of high stress-induced c-fos levels across the VLO (independent of viral vector group). Data from dorsal striatal regions are reported as percent immunoreactivity after thresholding. This method of quantification was selected over intensity measurements due to anatomical limitations, as white matter tracts may create low intensity fluorescence. All other regions are reported as mean intensity value. One to 3 images from VLO and MO per mouse, and 3–6 images from striatum were analyzed by an individual blinded to condition. Mean values were calculated per mouse, such that each mouse contributed a single value to analysis, reported as fold-change from the control mean.

Statistics and reproducibility

Response and magazine entry rates, photobeam breaks (i.e., locomotor counts), and tracer-filled cells were compared by ANOVA with repeating measures. Locomotor counts across 24 h and tracer-filled cell densities were subject to Greenhouse-Geisser corrections. Grooming counts in DREADD experiments were compared by unpaired one-tailed *t*-tests or ANOVA with repeating measures, as indicated. All other grooming counts and immunoblotting values were compared by unpaired *t*-tests or ANOVA as appropriate. Interaction effects permitted posthoc comparisons by paired or unpaired *t*-test as appropriate. $p \leq 0.05$ was considered significant. Sample sizes were based on past experiments. In the PIT experiment, the EB group was smaller than intended due to unexpected mouse attrition.

Two mice were excluded from the NAc retrograde tracer study due to incorrect infusion placement, resulting in final $n = 5$. Additionally, values exceeding 2 standard deviations from the mean were considered outliers. Outliers included 1 EB mouse in the reinforced session and 1 control mouse in the non-reinforced session in the initial figure, and those values were replaced by group means to avoid missing values in the repeated measures design. One control mouse from the 24 h locomotor behavior assay was repeatedly an outlier, and this mouse was omitted. One control value in the VLO PSD95 western blot was an outlier and was omitted. One EB mouse in the GAD67 pMO immunofluorescent analysis was an outlier and was omitted, as well as 1 control mouse that was an outlier in the GAD67 analysis in the aVLO, aMO, and pMO. This mouse was omitted from all GAD67 analyses. One EB mouse was an outlier in the DMS immunofluorescent striatin analysis and was omitted. Two control mice and 1 EB mouse in the amphetamine-elicited locomotion test were outliers and omitted from the analysis. One mouse was an outlier in the control group from the spray-elicited grooming of Gq-DREADD animals and was omitted.

Data availability

Data will be made available through the Emory University dataverse or by contacting the corresponding author.

Received: 14 May 2024; Accepted: 23 December 2024

Published online: 13 January 2025

References

1. Gremel, C. M. & Costa, R. M. Orbitofrontal and striatal circuits dynamically encode the shift between goal-directed and habitual actions. *Nat. Commun.* **4**, 2264. https://doi.org/10.1038/ncomms3264 (2013).
2. Li, D. C. et al. A molecularly integrated amygdalo-fronto-striatal network coordinates flexible learning and memory. *Nat. Neurosci.* **25**, 1213–1224. https://doi.org/10.1038/s41593-022-01148-9 (2022).
3. Zimmermann, K. S., Li, C. C., Rainnie, D. G., Ressler, K. J. & Gourley, S. L. Memory Retention involves the Ventrolateral Orbitofrontal Cortex: comparison with the Basolateral Amygdala. *Neuropsychopharmacology* **43**, 674. https://doi.org/10.1038/npp.2017.219 (2018).
4. Gourley, S. L. et al. The orbitofrontal cortex regulates outcome-based decision-making via the lateral striatum. *Eur. J. Neurosci.* **38**, 2382–2388. https://doi.org/10.1111/ejn.12239 (2013).
5. Hinton, E. A., Li, D. C., Allen, A. G. & Gourley, S. L. Social isolation in Adolescence disrupts cortical development and goal-dependent decision-making in Adulthood, despite Social Reintegration. *eNeuro* **6** https://doi.org/10.1523/ENEURO.0318-19.2019 (2019).
6. Ahmari, S. E. et al. Repeated cortico-striatal stimulation generates persistent OCD-like behavior. *Science* **340**, 1234–1239. https://doi.org/10.1126/science.1234733 (2013).
7. Morisot, N. et al. mTORC1 in the orbitofrontal cortex promotes habitual alcohol seeking. *Elife* **8**. https://doi.org/10.7554/eLife.51333 (2019).
8. Sequeira, M. K., Stachowicz, K. M., Seo, E. H., Yount, S. T. & Gourley, S. L. Cocaine disrupts action flexibility via glucocorticoid receptors. *iScience* **27**, 110148. https://doi.org/10.1016/j.isci.2024.110148 (2024).
9. Seabrook, L. T. et al. Disinhibition of the orbitofrontal cortex biases decision-making in obesity. *Nat. Neurosci.* **26**, 92–106. https://doi.org/10.1038/s41593-022-01210-6 (2023).
10. Cazares, C., Schreiner, D. C., Valencia, M. L. & Gremel, C. M. Orbitofrontal cortex populations are differentially recruited to support actions. *Curr. Biol.* **32**, 4675–4687. https://doi.org/10.1016/j.cub.2022.09.022 (2022). e4675.
11. Piantadosi, S. C., Chamberlain, B. L., Glausier, J. R., Lewis, D. A. & Ahmari, S. E. Lower excitatory synaptic gene expression in orbitofrontal cortex and striatum in an initial study of subjects with obsessive compulsive disorder. *Mol. Psychiatry* **26**, 986–998. https://doi.org/10.1038/s41380-019-0431-3 (2021).
12. Izquierdo, A. Functional heterogeneity within Rat Orbitofrontal cortex in reward learning and decision making. *J. Neurosci.* **37**, 10529–10540. https://doi.org/10.1523/JNEUROSCI.1678-17.2017 (2017).
13. Bradfield, L. A., Hart, G. & Balleine, B. W. Inferring action-dependent outcome representations depends on anterior but not posterior medial orbitofrontal cortex. *Neurobiol. Learn. Mem.* **155**, 463–473. https://doi.org/10.1016/j.nlm.2018.09.008 (2018).
14. Allen, A. T. et al. Inter-individual variability amplified through breeding reveals control of reward-related action strategies by Melanocortin-4 receptor in the dorsomedial striatum. *Commun. Biol.* **5**, 116. https://doi.org/10.1038/s42003-022-03043-2 (2022).
15. Burguiere, E., Monteiro, P., Mallet, L., Feng, G. & Graybiel, A. M. Striatal circuits, habits, and implications for obsessive-compulsive disorder. *Curr. Opin. Neurobiol.* **30**, 59–65. https://doi.org/10.1016/j.conb.2014.08.008 (2015).
16. Kalueff, A. V. et al. Neurobiology of rodent self-grooming and its value for translational neuroscience. *Nat. Rev. Neurosci.* **17**, 45–59. https://doi.org/10.1038/nrn.2015.8 (2016).
17. Monteiro, P. & Feng, G. Learning from animal models of obsessive-compulsive disorder. *Biol. Psychiatry*. **79**, 7–16. https://doi.org/10.1016/j.biopsych.2015.04.020 (2016).
18. Yount, S. T. et al. A molecularly defined orbitofrontal cortical neuron population controls compulsive-like behavior, but not inflexible choice or habit. *Prog Neurobiol.* **238**, 102632. https://doi.org/10.1016/j.pneurobio.2024.102632 (2024).
19. Yuste, R. & Bonhoeffer, T. Genesis of dendritic spines: insights from ultrastructural and imaging studies. *Nat. Rev. Neurosci.* **5**, 24–34. https://doi.org/10.1038/nrn1300 (2004).
20. Bourne, J. & Harris, K. M. Do thin spines learn to be mushroom spines that remember? *Curr. Opin. Neurobiol.* **17**, 381–386. https://doi.org/10.1016/j.conb.2007.04.009 (2007).
21. Barreiros, I. V., Panayi, M. C. & Walton, M. E. Organization of afferents along the anterior-posterior and medial-lateral axes of the rat Orbitofrontal Cortex. *Neuroscience* **460**, 53–68. https://doi.org/10.1016/j.neuroscience.2021.02.017 (2021).
22. Panayi, M. C. & Killcross, S. Functional heterogeneity within the rodent lateral orbitofrontal cortex dissociates outcome devaluation and reversal learning deficits. *Elife* **7**. https://doi.org/10.7554/eLife.37357 (2018).
23. Woon, E. P., Sequeira, M. K., Barbee, B. R. & Gourley, S. L. Involvement of the rodent prelimbic and medial orbitofrontal cortices in goal-directed action: a brief review. *J. Neurosci. Res.* **98**, 1020–1030. https://doi.org/10.1002/jnr.24567 (2020).
24. Fineberg, N. A. & Gale, T. M. Evidence-based pharmacotherapy of obsessive-compulsive disorder. *Int. J. Neuropsychopharmacol.* **8**, 107–129. https://doi.org/10.1017/S1461145704004675 (2005).
25. Zhang, K., Hill, K., Labak, S., Blatt, G. J. & Soghomonian, J. J. Loss of glutamic acid decarboxylase (Gad67) in Gpr88-expressing neurons induces learning and social behavior deficits in mice. *Neuroscience* **275**, 238–247. https://doi.org/10.1016/j.neuroscience.2014.06.020 (2014).
26. Benoist, M., Gaillard, S. & Castets, F. The striatin family: a new signaling platform in dendritic spines. *J. Physiol. Paris* **99**, 146–153. https://doi.org/10.1016/j.jphysparis.2005.12.006 (2006).
27. Welch, J. M., Wang, D. & Feng, G. Differential mRNA expression and protein localization of the SAP90/PSD-95-associated proteins (SAPAPs) in the nervous system of the mouse. *J. Comp. Neurol.* **472**, 24–39. https://doi.org/10.1002/cne.20060 (2004).
28. Balleine, B. W., Leung, B. K. & Ostlund, S. B. The orbitofrontal cortex, predicted value, and choice. *Ann. N Y Acad. Sci.* **1239**, 43–50. https://doi.org/10.1111/j.1749-6632.2011.06270.x (2011).
29. Parkes, S. L. et al. Insular and Ventrolateral Orbitofrontal cortices differentially contribute to goal-Directed Behavior in rodents. *Cereb. Cortex.* **28**, 2313–2325. https://doi.org/10.1093/cercor/bhx132 (2018).
30. Fresno, V., Parkes, S. L., Faugere, A., Coutureau, E. & Wolff, M. A thalamocortical circuit for updating action-outcome associations. *Elife* **8**. https://doi.org/10.7554/eLife.46187 (2019).
31. Cerpa, J. C., Marchand, A. R. & Coutureau, E. Distinct regional patterns in noradrenergic innervation of the rat prefrontal cortex. *J. Chem. Neuroanat.* **96**, 102–109. https://doi.org/10.1016/j.jchemneu.2019.01.002 (2019).
32. Murray, E. A., Moylan, E. J., Saleem, K. S., Basile, B. M. & Turchi, J. Specialized areas for value updating and goal selection in the primate orbitofrontal cortex. *Elife* **4**. https://doi.org/10.7554/eLife.11695 (2015).
33. Balleine, B. W. & O'Doherty, J. P. Human and rodent homologies in action control: corticostriatal determinants of goal-directed and habitual action. *Neuropsychopharmacology* **35**, 48–69. https://doi.org/10.1038/npp.2009.131 (2010).
34. Gillan, C. M., Robbins, T. W., Sahakian, B. J., van den Heuvel, O. A. & van Wingen, G. The role of habit in compulsivity. *Eur. Neuropsychopharmacol.* **26**, 828–840. https://doi.org/10.1016/j.euroneuro.2015.12.033 (2016).
35. Burguiere, E., Monteiro, P., Feng, G. & Graybiel, A. M. Optogenetic stimulation of lateral orbitofronto-striatal pathway suppresses compulsive behaviors. *Science* **340**, 1243–1246. https://doi.org/10.1126/science.1232380 (2013).
36. Stein, D. J. et al. Obsessive-compulsive disorder. *Nat. Rev. Dis. Primers.* **5**, 52. https://doi.org/10.1038/s41572-019-0102-3 (2019).
37. Lau, C. G. & Murthy, V. N. Activity-dependent regulation of inhibition via GAD67. *J. Neurosci.* **32**, 8521–8531. https://doi.org/10.1523/JNEUROSCI.1245-12.2012 (2012).

38. Lee, S. E., Lee, Y. & Lee, G. H. The regulation of glutamic acid decarboxylases in GABA neurotransmission in the brain. *Arch. Pharm. Res.* **42**, 1031–1039. https://doi.org/10.1007/s12272-019-01196-z (2019).
39. Manning, E. E., Geramita, M. A., Piantadosi, S. C., Pierson, J. L. & Ahmari, S. E. Distinct patterns of abnormal lateral Orbitofrontal cortex activity during compulsive grooming and reversal learning normalize after Fluoxetine. *Biol. Psychiatry* **93**, 989–999. https://doi.org/10.1016/j.biopsych.2021.11.018 (2023).
40. Takahashi, H. et al. Selective control of inhibitory synapse development by Slitrk3-PTPdelta trans-synaptic interaction. *Nat. Neurosci.* **15**, 389–398. https://doi.org/10.1038/nn.3040 (2012).
41. Sohal, V. S. & Rubenstein, J. L. R. Excitation-inhibition balance as a framework for investigating mechanisms in neuropsychiatric disorders. *Mol. Psychiatry* **24**, 1248–1257. https://doi.org/10.1038/s41380-019-0426-0 (2019).
42. Whyte, A. J. et al. Cell adhesion factors in the orbitofrontal cortex control cue-induced reinstatement of cocaine seeking and amygdala-dependent goal seeking. *J. Neurosci.* https://doi.org/10.1523/JNEUROSCI.0781-20.2021 (2021).
43. Lichtenberg, N. T. et al. Basolateral Amygdala to Orbitofrontal Cortex projections enable cue-triggered reward expectations. *J. Neurosci.* **37**, 8374–8384. https://doi.org/10.1523/JNEUROSCI.0486-17.2017 (2017).
44. Salin, P., Kachidian, P., Bartoli, M. & Castets, F. Distribution of striatin, a newly identified calmodulin-binding protein in the rat brain: an in situ hybridization and immunocytochemical study. *J. Comp. Neurol.* **397**, 41–59 (1998).
45. Li, D., Musante, V., Zhou, W., Picciotto, M. R. & Nairn, A. C. Striatin-1 is a B subunit of protein phosphatase PP2A that regulates dendritic arborization and spine development in striatal neurons. *J. Biol. Chem.* **293**, 11179–11194. https://doi.org/10.1074/jbc.RA117.001519 (2018).
46. Welch, J. M. et al. Cortico-striatal synaptic defects and OCD-like behaviours in Sapap3-mutant mice. *Nature* **448**, 894–900. https://doi.org/10.1038/nature06104 (2007).
47. Mailly, P., Aliane, V., Groenewegen, H. J., Haber, S. N. & Deniau, J. M. The rat prefrontostriatal system analyzed in 3D: evidence for multiple interacting functional units. *J. Neurosci.* **33**, 5718–5727. https://doi.org/10.1523/JNEUROSCI.5248-12.2013 (2013).
48. Hoover, W. B. & Vertes, R. P. Projections of the medial orbital and ventral orbital cortex in the rat. *J. Comp. Neurol.* **519**, 3766–3801. https://doi.org/10.1002/cne.22733 (2011).
49. Shih, C. W. & Chang, C. H. Anatomical analyses of collateral prefrontal cortex projections to the basolateral amygdala and the nucleus accumbens core in rats. *Brain Struct. Funct.* **229**, 97–114. https://doi.org/10.1007/s00429-023-02722-y (2024).
50. Lai, C. W., Shih, C. W. & Chang, C. H. Analysis of collateral projections from the lateral orbitofrontal cortex to nucleus accumbens and basolateral amygdala in rats. *J. Neurophysiol.* **127**, 1535–1546. https://doi.org/10.1152/jn.00127.2022 (2022).
51. Schilman, E. A., Uylings, H. B., Galis-de Graaf, Y., Joel, D. & Groenewegen, H. J. The orbital cortex in rats topographically projects to central parts of the caudate-putamen complex. *Neurosci. Lett.* **432**, 40–45. https://doi.org/10.1016/j.neulet.2007.12.024 (2008).
52. Zimmermann, K. S., Yamin, J. A., Rainnie, D. G., Ressler, K. J. & Gourley, S. L. Connections of the Mouse Orbitofrontal Cortex and regulation of goal-Directed Action selection by brain-derived neurotrophic factor. *Biol. Psychiatry* **81**, 366–377. https://doi.org/10.1016/j.biopsych.2015.10.026 (2017).
53. Lu, J. et al. Whole-brain mapping of direct inputs to dopamine D1 and D2 receptor-expressing medium spiny neurons in the posterior Dorsomedial Striatum. *eNeuro* **8**. https://doi.org/10.1523/ENEURO.0348-20.2020 (2021).
54. Feng, G. et al. Imaging neuronal subsets in transgenic mice expressing multiple spectral variants of GFP. *Neuron* **28**, 41–51. https://doi.org/10.1016/s0896-6273(00)00084-2 (2000).
55. Xu, P. et al. Double deletion of melanocortin 4 receptors and SAPAP3 corrects compulsive behavior and obesity in mice. *Proc. Natl. Acad. Sci. U S A* **110**, 10759–10764. https://doi.org/10.1073/pnas.1308195110 (2013).
56. Matsuno, H. et al. A naturally occurring null variant of the NMDA type glutamate receptor NR3B subunit is a risk factor of schizophrenia. *PLoS One.* **10**, e0116319. https://doi.org/10.1371/journal.pone.0116319 (2015).
57. Stirling, D. R. et al. CellProfiler 4: improvements in speed, utility and usability. *BMC Bioinform.* **22**, 433. https://doi.org/10.1186/s12859-021-04344-9 (2021).
58. Whyte, A. J. et al. Reward-related expectations trigger dendritic spine plasticity in the mouse Ventrolateral Orbitofrontal Cortex. *J. Neurosci.* **39**, 4595–4605. https://doi.org/10.1523/JNEUROSCI.2031-18.2019 (2019).
59. Gourley, S. L., Swanson, A. M. & Koleske, A. J. Corticosteroid-induced neural remodeling predicts behavioral vulnerability and resilience. *J. Neurosci.* **33**, 3107–3112. https://doi.org/10.1523/JNEUROSCI.2138-12.2013 (2013).
60. Radley, J. J., Anderson, R. M., Hamilton, B. A., Alcock, J. A. & Romig-Martin, S. A. Chronic stress-induced alterations of dendritic spine subtypes predict functional decrements in an hypothalamo-pituitary-adrenal-inhibitory prefrontal circuit. *J. Neurosci.* **33**, 14379–14391. https://doi.org/10.1523/JNEUROSCI.0287-13.2013 (2013).
61. Schneider, C. A., Rasband, W. S. & Eliceiri, K. W. NIH Image to ImageJ: 25 years of image analysis. *Nat. Methods* **9**, 671–675. https://doi.org/10.1038/nmeth.2089 (2012).
62. Paxinos, G. & Franklin, K. B. J. *The mouse brain in stereotaxic coordinates*. Compact 2nd edn. (Elsevier Academic Press, 2004).
63. Rosen, G. D. et al. RW. in *Int Mouse Genome Conference* Vol. 14, (2000).

Acknowledgements

This work was supported in part by NIH MH117103, DA044297, MH133740, and the Marcus Foundation. This work was also supported by the Emory University Integrated Cellular Imaging Core Facility (RRID: SCR_023534). The content is solely the responsibility of the authors and does not necessarily represent the official views of the National Institutes of Health. The Emory National Primate Research Center is supported by NIH OD011132. We thank members of the Gourley lab for their thoughtful discussions and feedback.

Author contributions

L.M.B., S.T.Y., A.T.A., E.H.S., A.M.S., and S.L.G. conducted experiments and analyzed their data. L.M.B. and S.L.G. composed the manuscript with contributions and editing by all other authors.

Declarations

Competing interests

The authors declare no competing interests.

Additional information

Supplementary Information The online version contains supplementary material available at https://doi.org/10.1038/s41598-024-84369-1.

Correspondence and requests for materials should be addressed to S.L.G.